

THE LUMINOSITY FUNCTION OF M DWARF STARS IN SELECTED AREA 109

G.N. MACE¹

Northern Arizona University, Summer REU student at Ball State

AND

T.M. JORDAN AND T.H. ROBERTSON

Department of Physics and Astronomy; Ball State University, Muncie, IN 47306

ABSTRACT

This paper presents the photometric luminosity classification of M dwarfs in Kaptyn's Selected Area 109 (SA109) as part of an ongoing program at Ball State University to probe low luminosity star contributions to the luminosity function. The reduction of data taken at the Southeastern Association for Research in Astronomy (SARA) telescope is still in the initial phases, but comparisons of this data to previous data from the National Undergraduate Research Observatory (NURO) and the Ball State Observatory (BSO) show that the classification results are consistent. With a limiting magnitude of $R=15.25$, we have observed nearly half of a square degree in SA109 and have detected approximately 74 percent of the expected M dwarfs, as determined by the luminosity function. The 26 M dwarfs which have been identified using R, I and CaH photometry, are confirmed using 2MASS J, H and K magnitudes. We present the detections of 17 ± 4.1 early type M dwarfs in half of SA109, compared to the expected value of 16 ± 4 for the entire region as determined the accepted luminosity function.

Subject headings: stars: luminosity function and mass function

1. INTRODUCTION

To understand Galactic structure it is essential to determine the luminosity function, of a large enough local region, so that we can accurately describe the history of the evolutionary process of the Milky Way. In order to find the luminosity function, the distribution and quantities of different spectral types throughout the Milky Way, it is necessary to complete a thorough stellar census. Many sky surveys, and standard lists, are dominated by high luminosity sources. This is due to the historical need for bright standards with shorter integration times, and greater fluxes. Thus, observations of low luminosity stars have been the increased focus of many astronomical programs in the recent years as instrumentation has improved and fainter limiting magnitudes have been attained.

The presence of CaH in the spectra of M dwarfs, and its absence in M giants, was first identified by Ohman (1934). This discrepancy is due to the lower surface pressure of the inflated giant, but its similar temperature to a dwarf. It was also determined that TiO is more abundant in M giants atmospheres than in M dwarfs (Ohman 1934). These observations agree with the restrictions on molecular environments established by Saha's equation. Thus, CaH can be used to differentiate between M dwarfs and M giants, as well as to probe surface gravity of M dwarfs (Mould & Wallis 1977).

Although the identification of M dwarfs using spectra is very useful it requires a large amount of observing time due to their low luminosity. This restricts the quantity that can be obtained in a single observing run. Since it is our goal to determine the luminosity function we need large samples and so we use intermediate-band photometry. By observing using an intermediate-band CaH filter, we are able to classify M dwarfs using CaH-r vs. R-I color-color plots (Robertson & Scott 2000 (RS2000), Matney et al. 2004). The observed

magnitudes are transformed to the Kron-Cousins system to allow for consistency with all previous data taken at at BSO and NURO (Robertson & Jordan 2005, RS2000).

It is the purpose of this program to identify variations in the luminosity function for Selected Areas both in and outside of the Galactic plane. Ball State became a member of SARA in the fall of 2005 and has only recently begun to reduce data from this telescope. Previous data will be easily compared to this new data since all observations have been transformed to the standard system. After the initial data is reduced, it is expected that any necessary changes to the observing method will be made and that large samples will be obtained to allow for greater statistical significance.

2. OBSERVATIONS AND DATA REDUCTION

2.1. Observations

Our data were obtained using an Apogee U42 camera on the SARA telescope at Kitt Peak National Observatory on June 7, 2007. The Apogee camera is a 2048×2048 pixel CCD which is thermoelectrically cooled to between $-17C$ and $-20C$. Our observations were taken using 2×2 binning to decrease both readout time and file size. This binning set the plate scale to $0.77''$ per pixel and the field of view to $13.14'$. Observations of standards were taken using the V,R,I,CaH, and B filters, and program fields were imaged through the R, I, and CaH filters.

We were able to image fields 109A through 109L giving us 12 of the 25 fields which comprise SA109. Our data gathering technique utilizes short, intermediate and long exposure sequences in all three filters. This ensures that the brightest sources are not over saturated in the short exposure sequence and that the fainter sources are detected with reasonable signal-to-noise in the long exposure sequence. The use of the intermediate exposure is to allow for further source matching between the short and long exposures which gives greater statistical significance to photometric values. Since the long CaH exposure is 720s, it was essential to have a stable guide

¹ Southeastern Association for Research in Astronomy (SARA) NSF-REU Summer Intern
Electronic address: gnm2@nau.edu

star for the field. In the event that a stable guide star could not be found, we instead acquired six 120 s images. The limiting magnitude for our observations is $m(R) \sim 15.25$ and was determined by plotting our observed R magnitudes against the corresponding error in those measurements.

2.2. Data Reduction

The data reduction process for this program utilized IRAF, MaxIm DL, and Microsoft Excel. The initial IRAF reduction was done with the standard procedure of computing master darks and bias frames through the use of *zerocombine* and *darkcombine*. The master flats were computed using *flatcombine* and the object frames were processed using *ccdproc*. In the event that a proper guide star could not be found, as described in §2.1, the six 120s CaH exposures were combined at this point using *imcombine*. Then, for detections above a 50 count threshold, *daofind* was used to compute coordinate files, as well as, magnitude files using *phot*. For these detections the $fwhm = 4$ and a source aperture of 14 pixels was used. To transform the R and I magnitudes to the standard Kron–Cousins system the standards were first fit to the Landolt catalog values (Landolt 1983,1992) using *fitparams*. Then, *invertfit* was used to transform the object magnitudes to the standard system using values that were determined from the standard observations. Sources which did not have matching detections in all three filters, but were in the same exposure sequence, were excluded since proper colors could not be computed by *fitparams*.

Using MaxIm DL, the world coordinate system(WCS) of each field was established by using *pinpoint astrometry*. In this step the long R exposure images were processed for each field since they have positions for all stars detected. After the installation of the *WCStools*² package in IRAF, *imstar* was used along with the coordinate file previously compiled by *daofind* to determine the $\alpha(2000)$ and $\delta(2000)$ of each detection.

The coordinate and magnitude data were then loaded into Excel. At this point a sorting protocol was established to 1) remove spurious detections between filters, 2) identify multiple detections of the same bright source, and 3) match detections between the three exposure length sequences for a single star. Treating each sequence separately, detections which were missing any magnitude or color values were removed. Then detections within 15 pixels of column 109 were eliminated, by sorting by physical X coordinates, since this column is non-responsive and leads to inaccurate photometry. Next, $\sigma(X)$ and $\sigma(Y)$ were computed for all detections in each filter. By removing all detections with σ greater than $2\sigma_{avg}$, all detections with spurious matches between filters were excluded. The WCS values determined by *imstar* were then added to the data sheet and physical coordinates were matched between photometric and astrometric detections. This match was made for all the detections in the long sequence and comparison of photometric and astrometric magnitudes for all twelve fields yields $\sigma_{avg}(R)=0.219$ magnitudes. Matches between the short, intermediate, and long exposures were made by comparison of physical coordinates as well as photometric values. The multiple detection photometry values were averaged and the σ was computed for the colors and magnitudes. For the matches in all 12 fields, $\sigma_{avg}(R)=0.043$, $\sigma_{avg}(CaH-r)=0.048$,

$$\sigma_{avg}(R-I)=0.038, \sigma_{avg}(CaH-r)=0.054.$$

Due to the fact that SARA data for this program is fairly new, there is no definite reduction procedure in place. Thus, some parts of the reduction process will likely be automated through the development of further IRAF protocol, as well as the extensive utilization of Excel macro's.

3. DATA AND RESULTS

3.1. Color–Color M Star Luminosity Classification

As explained in §1, the presence of CaH in the spectrum of a M star is a clear indicator that it is a dwarf. The photometric color–color plot in Figure 1 shows the difference between the dwarf and giant sequences. The dividing line is the location where the giant and dwarf loci diverge as has been previously determined by Dr. Robertson. To the left of this dividing line are stars of higher temperature where CaH can not be used to determine spectral class. To the right of this dividing line the M dwarf locus displays excess absorption in the CaH magnitude when compared to the giant locus. These data are sorted by the error in R–I, with the highest quality data ($\sigma(R-I) \leq 0.02$) directly correlated to the limiting magnitude of the project.

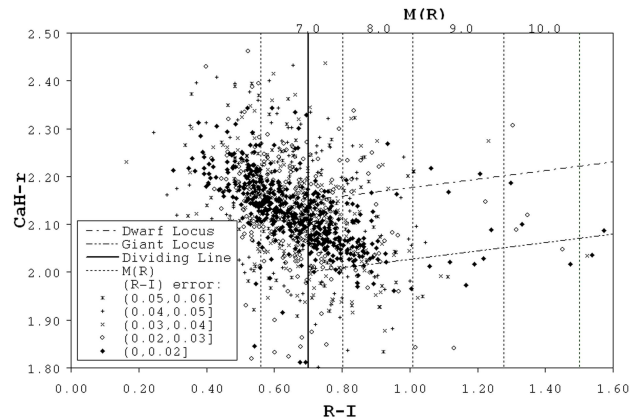


FIG. 1.— Color-color plot of SARA photometric detections in SA109 with giant and dwarf loci over-plotted.

Of particular interest, in the determination of the luminosity function, are the dividing lines which correspond to the integer ranges in absolute R magnitude. These ranges have been established using,

$$M_R = -6.862 + 61.375(R-I) - 108.875(R-I)^2 + 90.198(R-I)^3 - 27.468(R-I)^4$$

for $0.4 \leq (R-I) < 1.0$, and

$$M_R = -114.355 + 408.842(R-I) - 513.008(R-I)^2 + 286.537(R-I)^3 - 59.548(R-I)^4$$

for $1.0 \leq (R-I) < 1.5$, as determined by Siegel et al. (2002) and are overplotted in Figure 1. The luminosity function and photometric color indices from Cox (2000) were used by Robertson & Mason (2007) to compute the expected number of M dwarfs for each square degree to a limiting magnitude of $R=15$. Using this method Gregory Mace determined the values shown in the last column of Table 1 for a limiting magnitude of $R=15.25$.

² The WCStools is a package written and distributed by Doug Mink to establish, manipulate, and use WCS values. <http://tdc-www.harvard.edu/software/wcstools/>

TABLE 1
EXPECTED QUANTITIES FOR SA109 BASED ON MAIN SEQUENCE LUMINOSITY F

M(V)	Φ	M(R)	Spectral Type	d (pc)	Volume Sampled (pc ³)	Quantity Expected for 1 deg ² (R=15.25)
8	-2.41	6.90	K7	468	10373	40 ± 6.3
9	-2.32	7.72	M0	321	3341	16 ± 4.0
10	-2.14	8.50	M2	224	1137	8 ± 2.8
11	-1.99	9.35	—	151	351	4 ± 2.0
12	-1.82	10.2	M5	102	109	2 ± 1.4

REFERENCES. — Cox (2000)

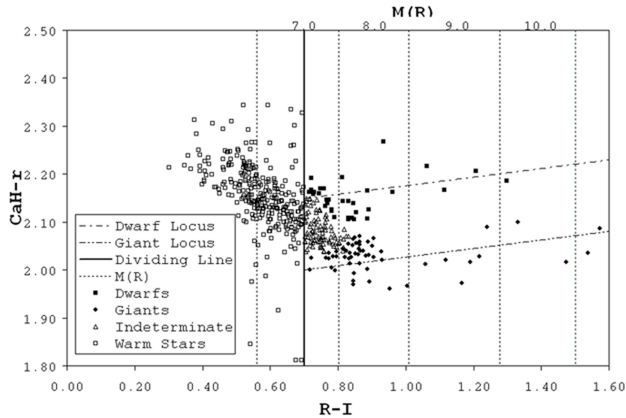


FIG. 2.— Color-color plot of $\sigma(R-I) \leq 0.02$ SARA photometric detections in SA109 with giant and dwarf loci over-plotted.

TABLE 2
MEASURED QUANTITIES
FOR M DWARFS IN SA109

R-I	M(R)	Quantity
0.728	7.20	6 ± 2.4
0.849	7.71	17 ± 4.1
1.036	8.52	2 ± 1.4
1.235	9.35	1 ± 1
1.460	10.2	0

Since the area surveyed in this paper is only for 12 of the 25 fields which comprise SA109, it is expected that approximately half as many detections would be found as is presented in Table 1. Plotting only the data for $\sigma(R-I) \leq 0.02$ in Figure 2, there are four distinct groups. The warmer stars, left of the dividing line, form an incomplete sample of the first magnitude range due to the ionization of CaH for $R-I < 0.70$. The giant and dwarf groups have been determined by their proximity to their corresponding loci. The indeterminate detections are within error margins of two or more determining limits, and thus could not be clearly classified. Table 2 presents the quantities which have been determined using the most probable M dwarf detections from Figure 2.

3.2. 2MASS Data

To better classify the M dwarfs, 2MASS data were compiled for all low error detections to the right of the dividing line in Figure 2. Matches were defined for all 2MASS detections as being within $3.6''$ (5 pixels) of our astrometric detections and having consistent photometry. Figure 3 is the color-color plot of the 2MASS data for our detections with the dwarf and giant loci overplotted (Bessell & Brett 1988). The dividing line has been predetermined by Dr. Robertson

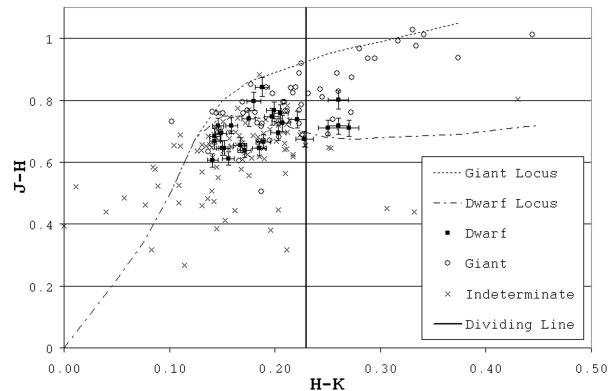


FIG. 3.— Color-color plot of 2MASS photometry for $\sigma(R-I) \leq 0.02$ detections with giant and dwarf loci over-plotted. Error bars of $\sigma_{avg} \approx 0.036$ are plotted for dwarf detections but are present for all points.

as the location where the giant and dwarf loci are not far enough apart to be discernible due to the average 2MASS error of ≈ 3.6 percent. This error has been plotted on the dwarf classifications to display their size, but are present for each point within the plot.

4. DISCUSSION

The data presented in Figure 2 show the distinctly separate colors of M giants and dwarfs. When the data are close to the dividing line, the difference is less obvious, and spurious classifications can occur if care is not taken. However, when grouping my data, to be plotted in Figure 3, I appear to have been overly strict in determining which stars in Figure 2 were dwarfs. This is evident by the large number of indeterminate detections which lie on, or very near, the dwarf locus in Figure 3 and may be M dwarfs. A further point by point comparison between Figures 2 and 3 will likely lead to better classification as well as a better determination of the dwarf and giant sequences near the dividing line in Figure 2.

Quantities which were presented in Table 2 are not exceedingly different from the expected values in Table 1. The quantities in Table 2 are generally within the expected error values that were determined using the accepted luminosity function. Since a detection is either a M dwarf, or it is not, Poisson statistics suggest an error of $\sqrt{\text{number detected}}$ and this accounts for differences in the bottom three rows. The quantity in the second row of Table 2 is high even after taking into account these errors, which leads to the conclusion that there are more M0 dwarfs in SA109 than is described by the accepted luminosity function. The first row of Table 2 is not near the expected value for a number of reasons. The greatest of these is that nearly half of the range in question is truncated by the

TABLE 3
DATA FOR MOST PROBABLE M DWARFS

Reduction ID	α (2000.0)	δ (2000.0)	R	M(R)	CaH	R-I	CaH-r	J	H	K	d (pc)
SA109L2-10	17:46:01.5	+00:03:36.82	13.245	7.546	14.932	0.814	2.144	11.239	10.472	10.273	138
SA109L3-47	17:46:29.529	+00:05:25.17	14.720	7.203	16.416	0.728	2.158	13.084	12.478	12.337	319
SA109E-34	17:46:38.817	-00:22:35.14	14.012	7.339	15.683	0.763	2.133	12.251	11.639	11.483	216
SA109E2-18	17:46:49.633	-00:23:32.44	13.343	7.320	15.050	0.758	2.169	11.577	10.931	10.781	160
SA109K2-21	17:47:00.943	+00:12:23.65	13.514	7.716	15.178	0.854	2.120	11.315	10.577	10.356	144
SA109E-20	17:47:06.615	-00:27:22.10	13.666	7.446	15.317	0.790	2.111	11.674	10.999	10.771	175
SA109K3-56	17:47:11.945	+00:07:21.22	14.976	7.861	16.690	0.887	2.166	12.749	11.952	11.772	265
SA109D2-23	17:47:12.834	-00:10:49.79	13.747	7.613	15.441	0.830	2.143	11.753	11.035	10.876	169
SA109C3-55	17:47:13.795	-00:05:20.56	14.944	7.622	16.605	0.832	2.105	13.199	12.544	12.377	291
SA109D-1	17:47:16.235	-00:14:59.91	12.117	7.857	13.781	0.886	2.107	9.818	9.017	8.757	71
SA109E-10	17:47:16.502	-00:27:47.22	13.167	7.413	14.832	0.782	2.126	11.171	10.478	10.329	141
SA109I2-11	17:47:29.858	+00:08:27.63	13.137	7.383	14.816	0.774	2.147	11.6	10.883	10.737	141
SA109F2-10	17:47:36.531	-00:30:15.27	13.329	7.367	15.003	0.770	2.139	11.331	10.605	10.398	156
SA109A3-77	17:47:43.745	-00:16:40.29	14.480	7.176	16.210	0.721	2.167	13.435	12.752	12.609	289
SA109A3-90	17:47:46.138	-00:07:38.70	15.028	7.210	16.755	0.730	2.163	13.372	12.705	12.562	366
SA109A3-79	17:47:51.097	-00:12:25.40	14.821	7.355	16.536	0.767	2.146	13.06	12.414	12.262	311
SA109B3-43	17:48:09.503	-00:05:24.63	14.468	8.199	16.212	0.962	2.163	12.053	11.295	11.09	179
SA109F3-61	17:48:11.589	-00:21:54.36	14.865	9.594	16.649	1.298	2.186	12.186	11.476	11.206	113
SA109G3-75	17:48:23.194	-00:28:35.50	14.859	7.618	16.507	0.831	2.108	13.293	12.45	12.262	281
SA109H2-24	17:48:25.730	-00:17:02.41	13.498	7.280	15.196	0.748	2.169	11.502	10.807	10.604	175
SA109H2-29	17:48:29.485	-00:11:54.82	13.769	7.677	15.448	0.845	2.139	11.812	11.071	10.896	165
SA109G3-41	17:48:35.953	-00:28:58.95	14.711	7.265	16.399	0.744	2.159	12.818	12.174	11.989	308
SA109I3-87	17:48:41.876	-00:06:24.89	15.051	8.073	16.870	0.934	2.268	12.936	12.189	11.992	249
SA109H-8	17:48:46.449	-00:17:49.65	13.197	7.660	14.846	0.841	2.109	11.013	10.302	10.052	128
SA109I2-11	17:48:54.041	-00:03:20.88	12.622	7.156	14.310	0.716	2.163	10.733	10.095	9.924	124
SA109I3-81	17:48:56.921	+00:00:33.69	14.976	8.875	16.715	1.114	2.167	12.635	11.918	11.658	166

dividing line in Figure 2, where CaH is ionized, and thus has been excluded. Another reason is due to the likely classification of dwarfs as indeterminate due to their close proximity to the other regions.

Overall, the data presented in this paper is a great initial probe of the application of this program's techniques to identifying M dwarfs with SARA observations. The values in Table 2, while not fully consistent, are of the same order of magnitude as the expected quantities in Table 1 and many are within the expected error. A full analysis of SA109, as well as follow-up individual classifications for each star, should further reduce selection error and yield more desirable results.

5. SUMMARY

The presence of CaH in the spectrum of a M star is a clear indicator that it is a dwarf. The determination of the number of dwarf stars of each absolute magnitude, in a given volume of space, establishes the luminosity function for that region and a knowledge of this is essential to our understanding of Galactic evolution. For SA109, which is near the galactic plane, the values of the luminosity function are of the same order of magnitude as would be expected by our current es-

timates of the luminosity function. The exception to this is early type M dwarfs which have a higher frequency than is expected. Yet, with such small numbers and high errors we can not be sure of our classification of this region as having an M dwarf excess until the entire region has been analyzed. The observation and reduction of data for other selected areas, within this program, will lead to better determinations of the luminosity function for low luminosity sources.

GM thanks Dr. Lisa Prato of Lowell Observatory for giving him a wealth of knowledge on data reduction, as well as an extremely helpful LaTeX example with which I was able to establish a format for this paper. Thanks to Matt Wood, Florida Institute of Technology, and SARA for this REU opportunity as well as the observing time to have taken the data presented here. This project was funded by a partnership between the National Science Foundation (NSF AST-0552798), Research Experiences for Undergraduates (REU), and the Department of Defense (DoD) ASSURE (Awards to Stimulate and Support Undergraduate Research Experiences) programs.

REFERENCES

- Barbuy, B., Schiavon, R.P., Gregorio-Hetem, J., Singh, P.D. & Batalha, C., 1993, *A&A*, 101, 409
 Bessell, M.S., & Brett, J.M., 1988, *PASP*, 100, 1134
 Cox, A.N. (ed), *Allen's Astrophysical Quantities*, 4th ed., 2000, 388 & 485
 Landolt, A.U., 1983, *AJ*, 88, 439
 Landolt, A.U., 1992, *AJ*, 104, 340
 Matney, J.E., Robertson, T.H., Jordan, T.M. et al., 2004, *BAAS* 136, 584
 Mould, J.R., & Wallis, R.E., 1977, *MNRAS*, 181, 625
 Ohman, Y., 1984, *ApJ*, 80, 171
 Robertson, T.H. & Furiak, N., 1995, *BAAS* 27, 1302 (abstract only)
 Robertson, T.H. & Scott, A., 2000, *BAAS* 32, 1392
 Robertson, T.H. & Jordan, T.M., 2004, *BAAS* 36, 1348
 Robertson, T.H. & Mason, J.R., 2007 (private communication)
 Siegel, M.H., Majewski, S.R., Reid, I.N., & Thompson, I.B., 2002, *ApJ*, 578, 151